Journal of Geoscience and Environment Protection, 2022, 10, 185-206
https://www.scirp.org/journal/gep
ISSN Online: 2327-4344
ISSN Print: 2327-4336

# Petro-Geochemistry Contraints of Côte d'Ivoire North-East Plutonites: Implications for Eoeburnean Magmatism of Baoulé-Mossi Domain (Southern of West African Craton)

**Brice Roland Kouassi[1*], Marc Ephrem Allialy[2], N'Guessan Houssou Nestor[2], Kouadio David Koffi[2]**

[1]UFR-Biological Sciences, Geosciences Department, Peleforo Gon Coulibaly University, Korhogo, Côte d'Ivoire
[2]Laboratory of Geology, Mineral and Energy Resources/Training and Research Unit in Earth Sciences and Mineral Resources, Félix Houphouët-Boigny University, Abidjan, Côte d'Ivoire
Email: *bricerolandk@gmail.com

**How to cite this paper:** Kouassi, B. R., Allialy, M. E., Nestor, N. H., & Koffi, K. D. (2022). Petro-Geochemistry Contraints of Côte d'Ivoire North-East Plutonites: Implications for Eoeburnean Magmatism of Baoulé-Mossi Domain (Southern of West African Craton). *Journal of Geoscience and Environment Protection, 10,* 185-206.
https://doi.org/10.4236/gep.2022.109012

**Received:** August 18, 2022
**Accepted:** September 26, 2022
**Published:** September 29, 2022



## Abstract

Plutonites are part of the set of crystallines compose the Precambrian basement. Their study is capital because it allows participating in the debates on the geodynamic evolution of the West African craton. This study concerns granitoids and dioritoids of the North-East of Côte d'Ivoire located in the Man-Leo ridge structured by Eoeburnean magmatism. The petrographic and geochemistry constraints make it possible to say that these rock formations have evolved by the process of fractional crystallization. They have a hybrid origin (mantle and crust), metaluminous to peraluminous highlighted by geochemistry. Concerning the geotectonic context, these plutonites of the Baoulé-Mossi domain are emplacement in a context of subduction more precisely in a context of volcanic arc.

## Keywords

Plutonites, Contraints, Magmatism, Source, Geotectonics, Côte d'Ivoire, West African Craton

## 1. Introduction

The West African Craton stabilized at ca. 1900 Ma and includes two principal Precambrian domains: the Réguibat Rise to the North and the Leo-Man Rise to the South (Rocci, 1965). The Leo-Man Rise is composed of an Archean cratonic nucleus in the southwest, the so-called Kéména-Man domain (KMD), surrounded by some Paleoproterozoic belts in the north and east forming the Baoulé-Mossi domain (**Figure 1**; Milési et al., 2004; Baratoux et al., 2011; Jessell et al., 2016). Based on new and historical U-Pb data, Parra-Avila et al. (2017) have identified continuous magmatic activity between ca. 2300 and 2000 Ma, highlighting a diachronous evolution across the Baoulé-Mossi domain. In this context, the tectonic evolution of the Baoulé-Mossi domain is divided into two main periods, the Eoeburnean phase between ca. 2260 and 2150 Ma and the Eburnean phase between ca. 2140 and 2050 Ma. During the Eoeburnean volcanic activity in the region occurred coevally with the emplacement of felsic intrusions across Burkina Faso and western Mali (Baratoux et al., 2011; de Kock et al., 2011; Feybesse et al., 2006; Lahondère et al., 2002; Tshibubudze et al., 2013). Generally, felsic intrusions from across the Baoulé-Mossi domain have been previously described as Paleoproterozoic chemical equivalents to Archean tonalite-trondhjemite-granodiorites (TTG) (Castaing et al., 2003; Doumbia et al., 1998; Egal et al., 2002; Gasquet et al., 2003; Lompo, 2009; Naba et al., 2004; Tapsoba et al., 2013; Vegas et al., 2008). The Baoulé-Mossi domain is made up of an association of mainly

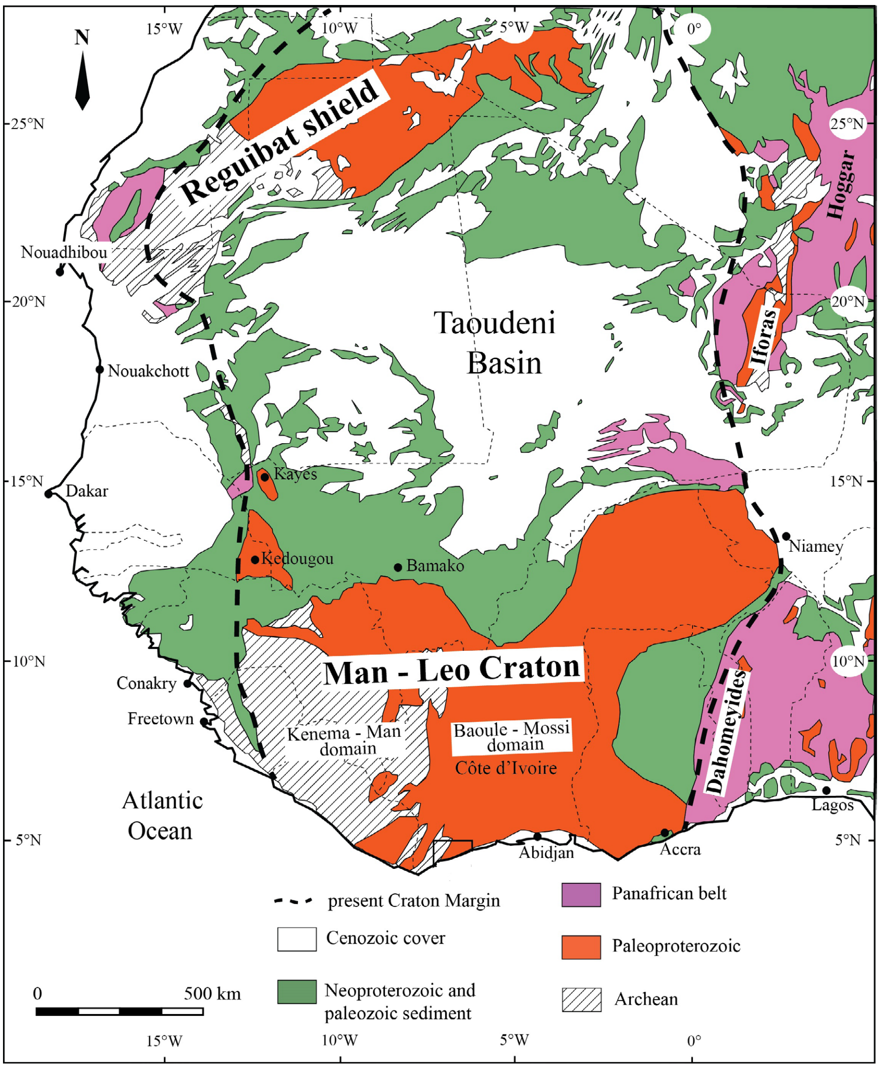


**Figure 1.** Simplified tectonic map of West African Craton (Grenholm, 2014).

low-grade Birimian (ca. 2.20-2.13 Ga) and Tarkwaian (ca. 2.10-2.09 Ga) sediments and plutono-volcanic rocks, which emplaced during a major juvenile crust-forming event, referred as the Eburnean orogeny and dated between ca. 2250 and 1980 Ma (Allibone et al., 2002; Feybesse et al., 2006; Pouclet et al., 2006; Vidal et al., 2009; Baratoux et al., 2011). Volcanic rocks' geochemical signature is compatible with the evolution from the tholeiitic oceanic crust or oceanic plateau to juvenile calc-alkaline volcanic island arcs (Abouchami et al., 1990; Leube et al., 1990; Boher et al., 1992; Baratoux et al., 2011). Eoeburnean intrusions dominate the eastern portion of the Baoulé-Mossi domain and during the Eburnean period, intrusions are mainly concentrated across the western portion. This study allows constraining the source and the geotectonic context of these plutonites. It is therefore a contribution to the Paleoproterozoic crustal evolution.

## 2. Local Geological Context

Located in the Paléoproterozoic field, geological formations in the Bondoukou region were structured during Eburnean orogenesis. The very open petrographic range of geological formation in the Bondoukou region and the complexity of structural phenomena make their study difficult. From a lithological point of view, the study area is covered by a complex set of geological formations. There are two major distinct fields: the quaternary domain (Holocene) and the Paleoproterozoic domain. Training in the quaternary field is the most recent in the Bondoukou region and has been deposited precisely at the Holocene (Zeade et al., 1995). They come from the alteration of the preexisting parent rock. There are two types:

- vases and sands: these are observable fluvial sediments only along rivers. These sediments have a wide lithological variety: more or less coarse sands, vases, and clays, fine and very fine silts (Zeade et al., 1995).
- Lateritic cuirass: Laterites refer to all indurated materials which constitute the soils, the superficial horizons as well as the deep horizons of the alteration profiles (Zeade et al., 1995). These often red or brown materials consisting of aluminum hydroxides and/or iron, come from the alteration of the rock without transport of minerals (residual rocks). These formations cover almost the surface of the study area and can be subdivided into three rock formations:
- Tarkwaïen formations;
- volcanic and sedimentary formations;
- Intrusive formations.

### 2.1. Tarkwaien Formations

This template has been tailored for output on the custom paper size (21 cm × 28.5 cm). The Tarkwaïen name is its origin in Ghana, named after the Ghanaian locality "Tarkwa". The arguments taken from the work carried out on the Tarkwaïen (Touré, 2007) are most often divergent. According to Touré (2007), the main reason for disagreements lies essentially in the existence of very little radiometric data on the formations attributed to Tarkwain. The Tarkwaïen ensemble of the Bondoukou region is essentially made up of conglomerate (met in the region of Duakouamé and Zanzan) and Cinérite (in the region of Takoutou and Siago). The presence of sandstone, quartz and Andesites is also reported by (Touré, 2007). The Tarkwaïen formations are based on the other Paleoproterozoic formations (Siméon et al., 1995), notably metavolcanites in the north, metasediments to the south and intrusive rocks (granodiorites, tonalites).

## 2.2. Volcanic and Sedimentary Formations

It is an intimate association of various volcanic rocks, pyroclastic rocks (fine conglomerates, tufs, etc.), clay sedimentary rocks and essentially chemical rocks (quartzite) (Zeade et al., 1995). So, this is a very complex formation for several geological units of a different petrographic nature. This set outcrops in the southern and northern regions of the study area with extensions to the East and West. The undifferentiated volcano-sedimentary shales the most encountered in this set constitute the large massif inside which is the whole sequence of volcanic and sedimentary hectometric lenses. Thus, for volcanic sets, metadolerites and metamicrogabbros which are massive rocks, with an isotropic appearance have a grainy and porphyroid texture with plagioclase or ferromagnesians. They are outcrop in several places in the formations of volcano-sedimentary schists. The amphibole and chlorite schists north of the Bondoukou granodiorite are dark-colored rocks and have a conglomeratic appearance with brecciated or angular elements (Zeade et al., 1995). On the north and west flanks of the Bondoukou granodiorite, outcrops metaandesites with porphyric microlithic texture. Besides these formations which occupy relatively large surfaces, there are also metagabbros, metarhyolites with a vitreous appearance. The sedimentary rocks are represented by calco-chlorito-schists who appear west of the Bondoukou granodiorite. It has a conglomerate aspect with more or less rounded and coarse elements. Small lenticles of quartz shale flip on the northern flank of the Bondoukou granodiorite. Volcano-sedimentary complexes are well marked in morphology and are present in all intrageosynclines. These formations were very studied everywhere in Côte d'Ivoire, given their genetic link with manganese mineralization, one of the first to work on the Birimien brought lithostratigraphic and individualized details within a volcano-sedimentary complex of detrital formations (quartzites, arkoses, sandstones) and terms plutono-volcanic (Andesites, gabbros, amphibolites).

## 2.3. Intrusive Formations

The intrusive formations in the Bondoukou region are the syntectonic granitoids and the post-tectonic intrusive granites (Tempier, 1969).

### 2.3.1. Syntectonic Granitoids

In these formations, undifferentiated metatonalites and metagranodiorites are the most widespread and are outcrop to the east, north and west of the study area. These formations with granonematoblastic texture, consisting of more or less sericitized oligoclase, xenomorphic quartz as well as Hornblende and green biotite (Zeade et al., 1995). Within the formations, we find:

- to the northeast: biotite metagranites which are medium-fine grain granites, light color containing both biotite and muscovite.
- to the northwest: granites and monzogranites with biotite. These fairly dark facies consist of more or less chloritized plagioclase and green biotite (Delor et al., 1995);
- to the west: a granodioritic facies whose rocks are melanocrats, these are biotite gran odiorites and/or hornblende with grainy texture with a percentage of plagioclase which dominates on that of the microcline.

### 2.3.2. Post-Tectonic Granitoids

Post-tectonic (discordant granites of Bondoukou type) which are outcrop northeast of the study area circumscribed around the city of Bondoukou, are essentially made up of biotite granodiorites and/or porphyroid texture. They cause contact metamorphism on the volcanic rocks. Most often isotropic in the central areas of the massif, their periphery presents ferromagnesians (biotite and hornblende) which are phenocrystals of plagioclase and individualize with them a mineral and/or high dip stretch to the NNW (Zeade et al., 1995). These rocks with melanocratic facies, give the impression of having been put in place after all folding and all metamorphism. With the work of (Touré et al., 1987), the traces of "Burkinian" orogenesis were highlighted in the Bondoukou region by the Rb-Sr age at 2166 ± 49 mA (on whole rock) of the porphyroid granodioritic facies of Bondoukou. This facies is a particular type of discordant and post-tectonic intrusive formation, hence the name of intrusive granite of the Bondoukou type attributed to the similar formations encountered in other regions of the country (Mankono, Dabakala, etc.). According to Touré (2007), the discordant granitoids of Bondoukou cannot be considered as younger than Baoulé type granitoids.

## 3. Analytical Methods

To obtain the results that will be presented in this study, we used two main methods.

The methodology consisted in observing and describing the different lithologies, either with the naked eye or using a magnifying glass on the ground. This phase was accompanied by samples. The samples collected allowed for the making of thin sections in the geochemical and geochronology laboratory of The University of Rennes 1. Their study was done in the geology, mineral and energy resources (LGRME) of the UFR Earth Sciences and the Mineral Resources (UFR STRM) of Félix Houphouët Boigny University of Abidjan-Cocody, Côte d'Ivoire.

This phase makes it possible to come out for each facies of rocks: color, texture, alteration levels, constitutive minerals (primary and secondary) and if possible, their proportions, the presence of sulfides and veins or venules of quartz and carbonate, etc. Its main objective was to identify geological formations in the area. In addition, to know their geotectonic protholites and contexts, geochemical analyzes on whole rock have also been carried out in the laboratory in Vancouver in Canada by fluorescence X (XRF) to dose the major elements ($SIO_2$, $AL_2O_3$, $Fe_2O_3$, MnO, MgO, CaO, $Na_2O$, $K_2O$, $TiO_2$ and $P_2O_5$) and ICP MS for the dosage of trace elements (As, Ba, Be, Cd , Co, Cr, CS, Cu, Ga, Ge, Hf, In, Mo, Nb, Nd, Ni, Pb, Rb, Sb, Sn, Sr, Ta, Th, U, V, W, Y and Zn) and rare earth elements (La, Ce, Pr, Nd, Sm, Eu, Gd, Tb, Dy, Ho, Er, Tm, Yb and Lu). For this geochemical study, 20 samples were selected (11 granitoids and 09 dioritoids).

## 4. Results

### 4.1. Petrography

Bondoukou plutonites are granitoids (granites, granodiorites and tonalites) and dioritoids (Gabbro and Diorites).

#### 4.1.1. Granite

These are medium grain rocks and leucocrats and of grainy texture. Macroscopic, they are made up of quartz, feldspar and biotite minerals (**Figure 2(A)**). On the microscope, the granites are made up of quartz crystals, generally altered

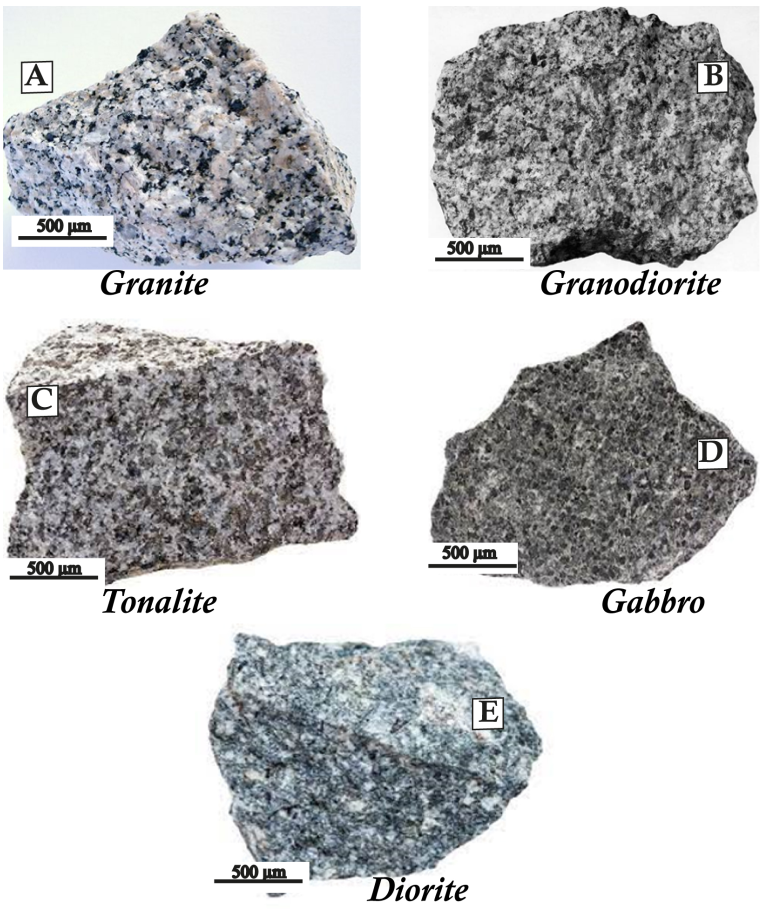


**Figure 2.** Granitoids and dioritoids of Bondoukou-Tanda region.

carbonate and sericite feldspars, and chlorite. Biotite is also present with Zircon inclusions and it shows on certain sections an alteration in chlorite. Preserved plagioclases are also observed, as well as rare sulfides and oxides.

#### 4.1.2. Granodiorite

The granodiorites are massive, weakly deformed and show medium to coarse grains (**Figure 2(B)**). They are made up of quartz, feldspaths, amphibole and biotite. These rocks often contain granophyres made up of quartz and feldspar; as well as enclosures of mafic rocks. Under the microscope, they show a grainy texture and are made up of Feldspaths minerals generally pseudomorphosed in sericite, epidote and carbonates. We also observe green hornblende, chlorite, preserved and zoned plagioclases, as well as rare sulfide.

#### 4.1.3. Tonalite

On the outcrop, the tonalite are medium and more or less mesocratic grains (**Figure 2(C)**). Macroscopically, we observe quartz crystals, feldspars, amphiboles and biotites. Microscopic observation, they show a grainy texture and are made up of microcline minerals, quartz, and orthoses. Feldspar crystals (plagioclase and/or alkaline) are often altered in carbonates, epidote and sericite. The observed chlorite comes from the pseudomorphosis of minerals of biotite and green hornblende. Rare sulphides as well as oxides are observed.

#### 4.1.4. Gabbro

The Gabbros are outcrop in the form of massifs, melanocrats, with a grainy texture (**Figure 2(D)**). The minerals observed are plagioclases and ferromagnesians. Under the microscope, the gabbros have a porphyric texture with pyroxene and green hornblende phenocrystals. Pyroxene crystals have generally undergone uralitization. Plagioclases are generally pseudomorphosed in carbonates (calcite ± dolomie). Gabbros also contain chlorite, epidote, sericite, sulfides and oxides. We also observe quartzo-feldspathetic venules often associated with epidot crystals.

#### 4.1.5. Diorite

The facies of diorite are mesocrats, of average granulometry and generally in enclaves of granitoids (**Figure 2(E)**). They are dominated by two minerals of Plagioclase and green hornblende. Under the microscope, these rocks show a grainy texture. They are generally made up of green hornblendes and plagioclase; and accessory epidote, chlorite and sericite. So, let's note the presence of rare sulfides and oxides.

### 4.2. Geochemistry

The results of intrusive analyzes are recorded in **Tables 1-3**. Inserted into the classification diagram of (Middlemost, 1994) applied to plutonites the samples are distributed from the fields of Tonalites to granites via the granodiorites (**Figure 3(A)**) as well as gabbros and diorites (**Figure 4(A)**). Reported to the

**Table 1.** Major (%) and trace (ppm) element composition of Bondoukou-Tanda region plutonites.

| Ref Echantillon | Granodiorite | Granodiorite | Granodiorite | Granodiorite | Granodiorite | Granodiorite | Granodiorite | Granodiorite |
|---|---|---|---|---|---|---|---|---|
| | **TA 010** | **TA 011** | **TA 019** | **TA 020** | **TA 026** | **TB 002** | **TB 023** | **TB 007** |
| **$SiO_2$** | 67.25 | 67.60 | 68.70 | 69.36 | 68.56 | 68.79 | 66.81 | 69.98 |
| **$Al_2O_3$** | 15.09 | 15.39 | 14.65 | 15.20 | 14.77 | 15.43 | 14.9 | 14.77 |
| **$Fe_2O_3$** | 4.15 | 3.87 | 4.51 | 3.28 | 4.06 | 3.04 | 4.28 | 2.65 |
| **MnO** | 0.06 | 0.05 | 0.06 | 0.04 | 0.07 | 0.05 | 0.06 | 0.05 |
| **MgO** | 1.69 | 1.57 | 1.41 | 1.04 | 1.73 | 0.96 | 1.65 | 0.81 |
| **CaO** | 3.84 | 2.50 | 3.06 | 2.87 | 3.70 | 2.99 | 3.32 | 2.41 |
| **$Na_2O$** | 4.50 | 4.41 | 4.19 | 5.05 | 4.37 | 5.33 | 4.36 | 4.68 |
| **$K_2O$** | 1.50 | 1.98 | 1.60 | 1.65 | 1.62 | 1.28 | 1.54 | 2.59 |
| **$TiO_2$** | 0.42 | 0.40 | 0.38 | 0.33 | 0.42 | 0.32 | 0.39 | 0.27 |
| **$P_2O_5$** | 0.18 | 0.14 | 0.15 | 0.14 | 0.15 | 0.12 | 0.12 | 0.1 |
| **Total** | **100.22** | **99.68** | **100.19** | **100.25** | **100.51** | **99.4** | **99.04** | **99.17** |
| **La** | 20.22 | 30.09 | 13.53 | 135.4 | 16.9 | 28.2 | 15.6 | 22.6 |
| **Ce** | 43.56 | 47.79 | 34.74 | 85.52 | 35.16 | 55.3 | 36.7 | 45.3 |
| **Nd** | 20.27 | 25.92 | 14.85 | 108.3 | 15.87 | 22.3 | 15.3 | 17.8 |
| **Pr** | 5.245 | 6.786 | 3.76 | 27.22 | 4.105 | 6.16 | 3.88 | 5.08 |
| **Sm** | 3.539 | 4.355 | 2.706 | 19.38 | 2.802 | 3.63 | 2.54 | 3.02 |
| **Eu** | 1.012 | 1.249 | 0.857 | 5.524 | 0.862 | 1.04 | 0.8 | 0.83 |
| **Gd** | 2.503 | 3.381 | 1.917 | 18.34 | 2.167 | 3.01 | 2.14 | 2.24 |
| **Tb** | 0.318 | 0.463 | 0.265 | 2.378 | 0.288 | 0.34 | 0.26 | 0.27 |
| **Dy** | 1.648 | 2.413 | 1.349 | 11.81 | 1.514 | 1.71 | 1.39 | 1.38 |
| **Ho** | 0.29 | 0.442 | 0.244 | 2.019 | 0.273 | 0.28 | 0.26 | 0.22 |
| **Er** | 0.76 | 1.19 | 0.634 | 4.871 | 0.763 | 0.79 | 0.73 | 0.69 |
| **Tm** | 0.109 | 0.171 | 0.099 | 0.655 | 0.115 | 0.13 | 0.11 | 0.11 |
| **Yb** | 0.741 | 1.105 | 0.666 | 3.832 | 0.734 | 0.72 | 0.78 | 0.74 |
| **Lu** | 0.108 | 0.168 | 0.102 | 0.553 | 0.118 | 0.12 | 0.11 | 0.12 |
| **Ba** | 322 | 530 | 364.7 | 358.2 | 315.1 | 380 | 312 | 665 |
| **Be** | 0.901 | 1.06 | 0.98 | 1.744 | 0.93 | 3 | 3 | 3 |
| **Cd** | <L.D. | 0.137 | 0.168 | 0.178 | 0.159 | <0.1 | <0.1 | <0.1 |
| **Co** | 11.5 | 10.58 | 11.15 | 9.238 | 12.37 | 6.5 | 10.7 | 6 |
| **Cr** | 214.5 | 226.5 | 360.7 | 343.2 | 154.1 | | | |
| **Cs** | 0.566 | 0.759 | 0.652 | 0.907 | 0.629 | 1.7 | 0.8 | 1.4 |
| **Cu** | 44.57 | 45.86 | 32.56 | 11.61 | 27.06 | 24.7 | 32.6 | 9.7 |
| **Ga** | 19.27 | 19.72 | 19.19 | 20.72 | 18.73 | 19.7 | 17.1 | 16.5 |
| **Ge** | 0.908 | 0.935 | 0.949 | 1.07 | 1.072 | | | |
| **Hf** | 2.778 | 3.259 | 3.383 | 3.337 | 3.036 | 3.2 | 3 | 2.9 |

Continued

| | | | | | | | | |
|---|---|---|---|---|---|---|---|---|
| **Mo** | 1.275 | 1.468 | 2.323 | 2.112 | 0.936 | 0.1 | 0.1 | 0.2 |
| **Nb** | 5.528 | 4.236 | 3.876 | 3.566 | 4.408 | 4 | 4 | 5.3 |
| **Ni** | 34.52 | 30.74 | 38.96 | 27.75 | 37.2 | 8.5 | 22.7 | 7.5 |
| **Pb** | 4.2595 | 4.8311 | 6.4487 | 9.1577 | 4.6234 | 1.5 | 1.9 | 4.3 |
| **Rb** | 40.27 | 45.27 | 42.18 | 52.48 | 42.83 | 45.6 | 48.8 | 88.5 |
| **Sc** | 8.04 | 7.17 | 7.53 | 5.18 | 8.12 | | | |
| **Sn** | 0.668 | 0.67 | 0.797 | 0.803 | 0.567 | <1 | <1 | <1 |
| **Sr** | 525.2 | 448.1 | 457.7 | 623.3 | 413 | 723.6 | 402.6 | 587.2 |
| **Ta** | 0.807 | 0.459 | 0.412 | 0.339 | 0.56 | 0.6 | 0.4 | 0.5 |
| **Th** | 2.635 | 2.863 | 3.378 | 5.246 | 2.886 | 3.3 | 2.8 | 4.9 |
| **U** | 0.793 | 0.993 | 0.998 | 2.571 | 0.866 | 1.3 | 0.6 | 1.7 |
| **Y** | 8.547 | 13.13 | 6.413 | 63.71 | 8.461 | 8.9 | 7.9 | 7.9 |
| **Zn** | 59.21 | 55.24 | 54.5 | 66.94 | 58.44 | 39 | 36 | 38 |
| **Zr** | 111.8 | 135.1 | 138.7 | 127.1 | 121.1 | 117.3 | 116.9 | 102.4 |

**Table 2.** Major (%) and trace (ppm) element composition of Bondoukou-Tanda region plutonites.

| **Ref Echantillon** | **Granite** | **Granite** | **Tonalite** |
|---|---|---|---|
| | **TA 048** | **TA 007** | **TA 033** |
| **$SiO_2$** | 76.13 | 72.81 | 61.49 |
| **$Al_2O_3$** | 12.68 | 11.18 | 15.78 |
| **$Fe_2O_3$** | 1.59 | 5.92 | 6.02 |
| **MnO** | 0.63 | 0.09 | 0.08 |
| **MgO** | 0.07 | 1.43 | 2.27 |
| **CaO** | 0.48 | 2.63 | 4.79 |
| **$Na_2O$** | 4.28 | 2.70 | 4.57 |
| **$K_2O$** | 3.94 | 1.23 | 1.36 |
| **$TiO_2$** | 0.09 | 0.59 | 0.58 |
| **$P_2O_5$** | 0.05 | 0.09 | 0.20 |
| **PF** | 0.49 | 1.59 | 1.56 |
| **Total** | **100.43** | **100.24** | 98.69 |
| **La** | 16.73 | 27.33 | 17.8 |
| **Ce** | 27.43 | 51.61 | 37.99 |
| **Nd** | 9.771 | 20.05 | 18.57 |
| **Pr** | 2.864 | 5.553 | 4.615 |
| **Sm** | 1.501 | 3.385 | 3.587 |
| **Eu** | 0.348 | 0.93 | 1.082 |

Continued

| | | | |
|---|---|---|---|
| **Gd** | 1.052 | 2.911 | 2.752 |
| **Tb** | 0.125 | 0.436 | 0.374 |
| **Dy** | 0.61 | 2.581 | 1.969 |
| **Ho** | 0.096 | 0.496 | 0.359 |
| **Er** | 0.284 | 1.349 | 0.975 |
| **Tm** | 0.04 | 0.207 | 0.137 |
| **Yb** | 0.326 | 1.34 | 0.891 |
| **Lu** | 0.063 | 0.203 | 0.138 |
| **As** | 1.704 | <L.D. | 2.667 |
| **Ba** | 143.9 | 235.2 | 403.2 |
| **Be** | 1.816 | 0.824 | 0.979 |
| **Bi** | <L.D. | <L.D. | <L.D. |
| **Cd** | 0.601 | <L.D. | 0.148 |
| **Co** | 10.35 | 16.37 | 18.13 |
| **Cr** | 254 | 233.9 | 257.4 |
| **Cs** | 0.82 | 0.676 | 0.705 |
| **Cu** | 21.41 | 27.43 | 36.84 |
| **Ga** | 21.1 | 13.67 | 21.7 |
| **Ge** | 1.467 | 1.084 | 1.05 |
| **Hf** | 3.181 | 2.46 | 1.535 |
| **Mo** | 2.911 | 1.414 | 3.403 |
| **Nb** | 4.108 | 7.76 | 41.17 |
| **Ni** | 13.16 | 34.32 | 5.2048 |
| **Pb** | 10.9496 | 4.6343 | 41.63 |
| **Rb** | 122.9 | 33.13 | 10.9 |
| **Sc** | 2.63 | 12.36 | <L.D. |
| **Sn** | <L.D. | 0.812 | 0.649 |
| **Sr** | 76.61 | 183.6 | 708.9 |
| **Ta** | 0.445 | 1.163 | 0.278 |
| **Th** | 15.9 | 4.049 | 2.126 |
| **U** | 2.799 | 0.875 | 0.796 |
| **V** | 18.89 | 102.7 | 93.35 |
| **Y** | 3.131 | 14.87 | 10.36 |
| **Zn** | 19.92 | 45.54 | 79.42 |
| **Zr** | 77.85 | 98.35 | 130 |

**Table 3.** Major (%) and trace (ppm) element composition of Bondoukou-Tanda region plutonites.

| Ref Echantillon | TA 010 | TA 011 | TA 019 | TA 020 | TA 026 | TB 002 | TB 023 | TB 007 |
|---|---|---|---|---|---|---|---|---|
| $SiO_2$ | 67.25 | 67.60 | 68.70 | 69.36 | 68.56 | 68.79 | 66.81 | 69.98 |
| $Al_2O_3$ | 15.09 | 15.39 | 14.65 | 15.20 | 14.77 | 15.43 | 14.9 | 14.77 |
| $Fe_2O_3$ | 4.15 | 3.87 | 4.51 | 3.28 | 4.06 | 3.04 | 4.28 | 2.65 |
| MnO | 0.06 | 0.05 | 0.06 | 0.04 | 0.07 | 0.05 | 0.06 | 0.05 |
| MgO | 1.69 | 1.57 | 1.41 | 1.04 | 1.73 | 0.96 | 1.65 | 0.81 |
| CaO | 3.84 | 2.50 | 3.06 | 2.87 | 3.70 | 2.99 | 3.32 | 2.41 |
| $Na_2O$ | 4.50 | 4.41 | 4.19 | 5.05 | 4.37 | 5.33 | 4.36 | 4.68 |
| $K_2O$ | 1.50 | 1.98 | 1.60 | 1.65 | 1.62 | 1.28 | 1.54 | 2.59 |
| $TiO_2$ | 0.42 | 0.40 | 0.38 | 0.33 | 0.42 | 0.32 | 0.39 | 0.27 |
| $P_2O_5$ | 0.18 | 0.14 | 0.15 | 0.14 | 0.15 | 0.12 | 0.12 | 0.1 |
| PF | 1.54 | 1.78 | 1.51 | 1.30 | 1.06 | 1.04 | 1.56 | 0.78 |
| **Total** | **100.22** | **99.68** | **100.19** | **100.25** | **100.51** | **99.4** | **99.04** | **99.17** |
| La | 20.22 | 30.09 | 13.53 | 135.4 | 16.9 | 28.2 | 15.6 | 22.6 |
| Ce | 43.56 | 47.79 | 34.74 | 85.52 | 35.16 | 55.3 | 36.7 | 45.3 |
| Nd | 20.27 | 25.92 | 14.85 | 108.3 | 15.87 | 22.3 | 15.3 | 17.8 |
| Pr | 5.245 | 6.786 | 3.76 | 27.22 | 4.105 | 6.16 | 3.88 | 5.08 |
| Sm | 3.539 | 4.355 | 2.706 | 19.38 | 2.802 | 3.63 | 2.54 | 3.02 |
| Eu | 1.012 | 1.249 | 0.857 | 5.524 | 0.862 | 1.04 | 0.8 | 0.83 |
| Gd | 2.503 | 3.381 | 1.917 | 18.34 | 2.167 | 3.01 | 2.14 | 2.24 |
| Tb | 0.318 | 0.463 | 0.265 | 2.378 | 0.288 | 0.34 | 0.26 | 0.27 |
| Dy | 1.648 | 2.413 | 1.349 | 11.81 | 1.514 | 1.71 | 1.39 | 1.38 |
| Ho | 0.29 | 0.442 | 0.244 | 2.019 | 0.273 | 0.28 | 0.26 | 0.22 |
| Er | 0.76 | 1.19 | 0.634 | 4.871 | 0.763 | 0.79 | 0.73 | 0.69 |
| Tm | 0.109 | 0.171 | 0.099 | 0.655 | 0.115 | 0.13 | 0.11 | 0.11 |
| Yb | 0.741 | 1.105 | 0.666 | 3.832 | 0.734 | 0.72 | 0.78 | 0.74 |
| Lu | 0.108 | 0.168 | 0.102 | 0.553 | 0.118 | 0.12 | 0.11 | 0.12 |
| Ba | 322 | 530 | 364.7 | 358.2 | 315.1 | 380 | 312 | 665 |
| Be | 0.901 | 1.06 | 0.98 | 1.744 | 0.93 | 3 | 3 | 3 |
| Cd | <L.D. | 0.137 | 0.168 | 0.178 | 0.159 | <0.1 | <0.1 | <0.1 |
| Co | 11.5 | 10.58 | 11.15 | 9.238 | 12.37 | 6.5 | 10.7 | 6 |
| Cr | 214.5 | 226.5 | 360.7 | 343.2 | 154.1 | | | |
| Cs | 0.566 | 0.759 | 0.652 | 0.907 | 0.629 | 1.7 | 0.8 | 1.4 |
| Cu | 44.57 | 45.86 | 32.56 | 11.61 | 27.06 | 24.7 | 32.6 | 9.7 |
| Ga | 19.27 | 19.72 | 19.19 | 20.72 | 18.73 | 19.7 | 17.1 | 16.5 |

**Continued**

| | | | | | | | | |
|---|---|---|---|---|---|---|---|---|
| Ge | 0.908 | 0.935 | 0.949 | 1.07 | 1.072 | | | |
| Hf | 2.778 | 3.259 | 3.383 | 3.337 | 3.036 | 3.2 | 3 | 2.9 |
| Mo | 1.275 | 1.468 | 2.323 | 2.112 | 0.936 | 0.1 | 0.1 | 0.2 |
| Nb | 5.528 | 4.236 | 3.876 | 3.566 | 4.408 | 4 | 4 | 5.3 |
| Ni | 34.52 | 30.74 | 38.96 | 27.75 | 37.2 | 8.5 | 22.7 | 7.5 |
| Pb | 4.2595 | 4.8311 | 6.4487 | 9.1577 | 4.6234 | 1.5 | 1.9 | 4.3 |
| Rb | 40.27 | 45.27 | 42.18 | 52.48 | 42.83 | 45.6 | 48.8 | 88.5 |
| Sc | 8.04 | 7.17 | 7.53 | 5.18 | 8.12 | | | |
| Sn | 0.668 | 0.67 | 0.797 | 0.803 | 0.567 | <1 | <1 | <1 |
| Sr | 525.2 | 448.1 | 457.7 | 623.3 | 413 | 723.6 | 402.6 | 587.2 |
| Ta | 0.807 | 0.459 | 0.412 | 0.339 | 0.56 | 0.6 | 0.4 | 0.5 |
| Th | 2.635 | 2.863 | 3.378 | 5.246 | 2.886 | 3.3 | 2.8 | 4.9 |
| U | 0.793 | 0.993 | 0.998 | 2.571 | 0.866 | 1.3 | 0.6 | 1.7 |
| Y | 8.547 | 13.13 | 6.413 | 63.71 | 8.461 | 8.9 | 7.9 | 7.9 |
| Zn | 59.21 | 55.24 | 54.5 | 66.94 | 58.44 | 39 | 36 | 38 |
| Zr | 111.8 | 135.1 | 138.7 | 127.1 | 121.1 | 117.3 | 116.9 | 102.4 |

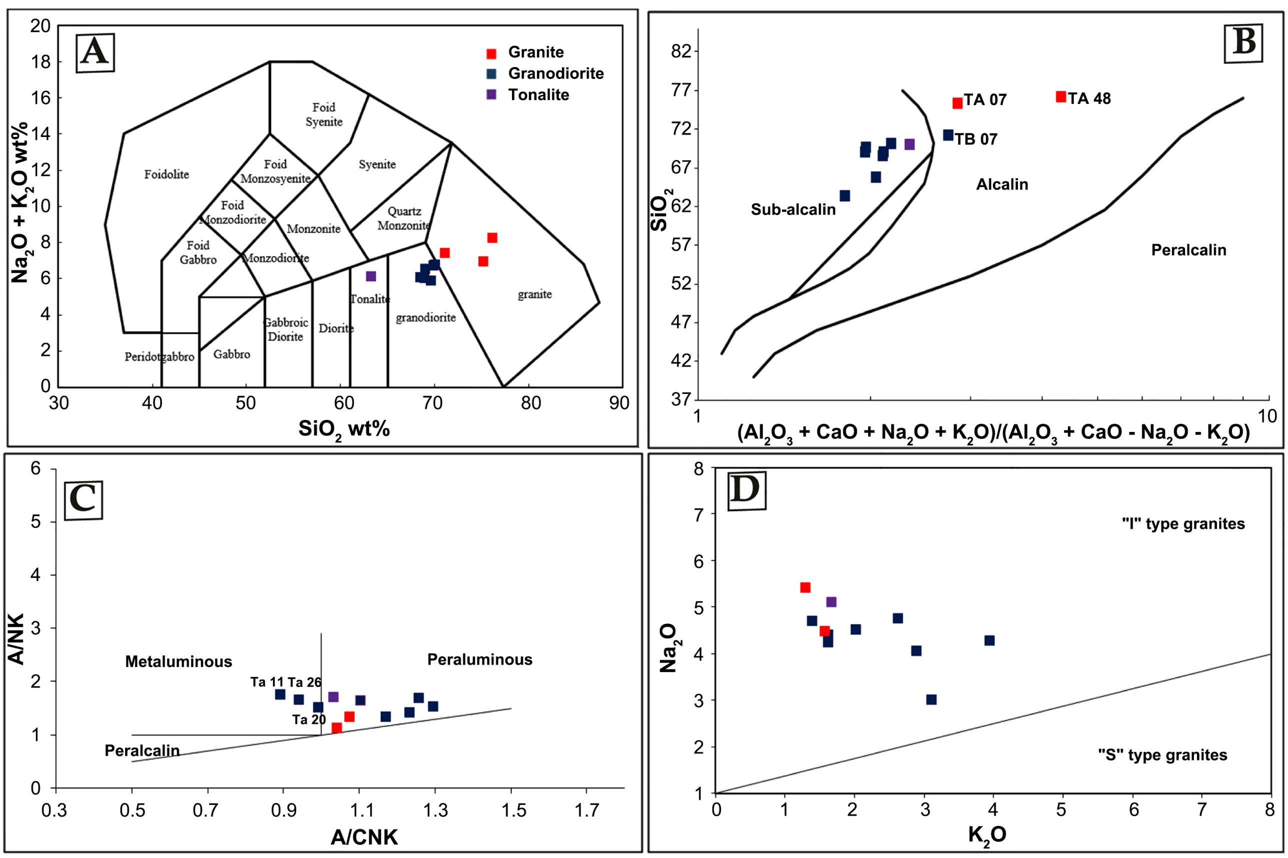


**Figure 3.** (A) Classification diagram from Middlemost (1994); (B) Diagram of Wright et al. (1969); (C) Diagram of Shand (1922) and (D) Diagram of Chappell & White (1974) applied to the granitoids of the Bondoukou-Tanda region.

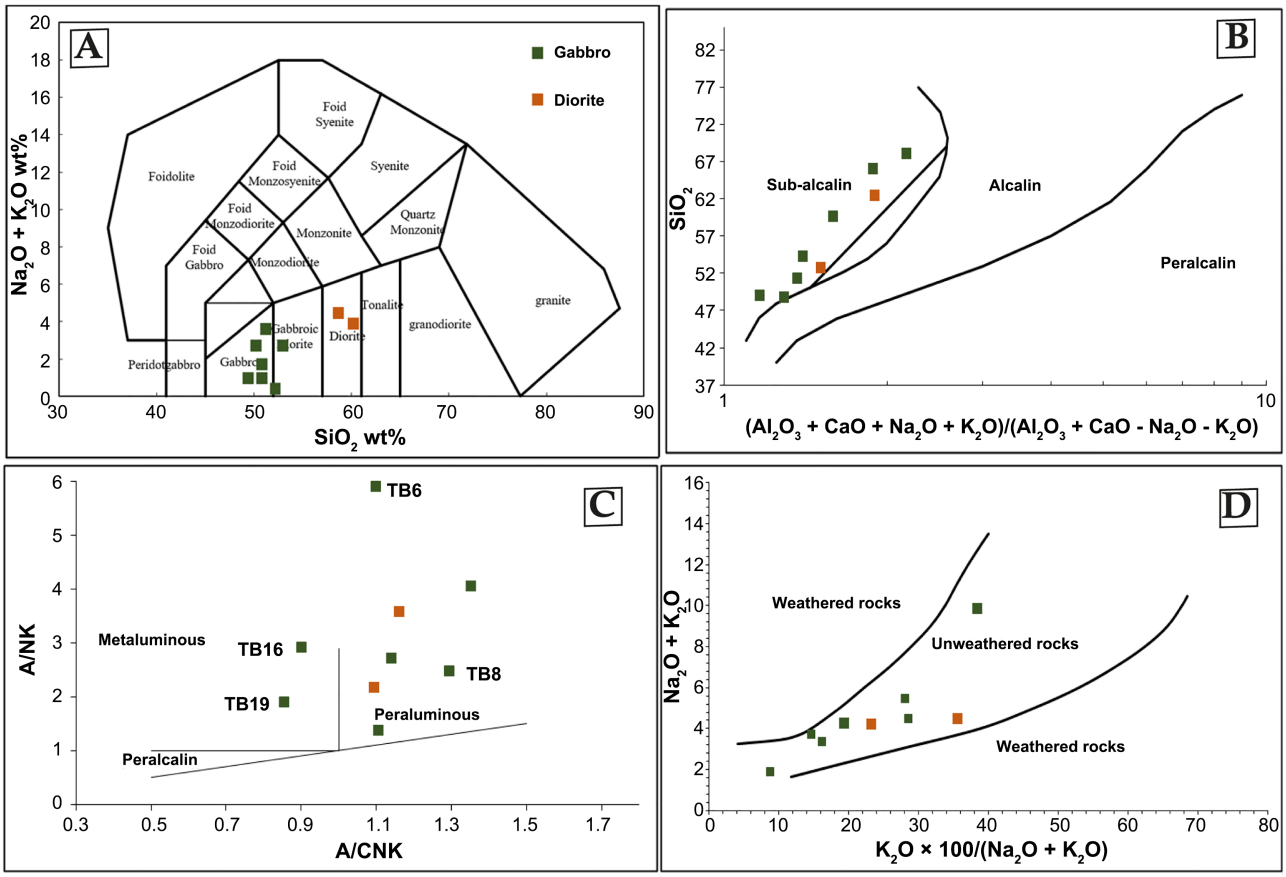


Figure 4. (A) Classification diagram from Middlemost (1994); (B) Diagram of Wright et al. (1969); (C) Diagram of Shand (1922) and (D) Diagram of Chappell & White (1974) applied to the granitoids of the Bondoukou-Tanda region.

diagram of (Wright et al., 1969) (Figure 3(B) and Figure 4(B)), the intrusive of the Bondoukou region shows a chimism generally identical to that of sub-alkaline rocks. However, it should be noted that the TB 07 granodiorite sample as well as the granites TA 07 and TA 48 show alkaline chemicals. The diagram of (Shand, 1922) (Figure 3(C) and Figure 4(C)), indicates that these rocks are metaluminous to pearluminous. The granitoides and dioritoides of Bondoukou region are type I (Figure 3(D)) and unweathered rocks (Figure 4(D)).

#### 4.2.1. Granite

$SiO_2$ and alkaline contents ($Na_2O + K_2O$) of granites vary from 75.25% to 76.18% and from 6.94% to 8.23%. Their contents in $Al_2O_3$ and MgO vary respectively from 12.68% to 13.13% and from 0.07% to 0.38%, with (Mg#) = 8.47 to 23.96. Their $TiO_2$ value is very low (0.09% to 0.18%). The granites define a calco-alkaline chemical (Figure 3(B)). The REE contents (ΣREE) of the granites are between 61.24 ppm and 68.10 ppm. The spectrum of the REE of these rocks normalized to chondrites according to (Sun & Mc. Donough, 1995), presented to (Figure 5(A)) with average slope with an average fractionation: [$(La/Sm)_N$ = 5.47 - 6.79; $(La/Yb)_N$ = 30.81 - 33.89]. These rocks generally have a negative anomaly to positive in Europium (Eu/Eu* = 0.86 - 1.84), probably due to a divergence in the

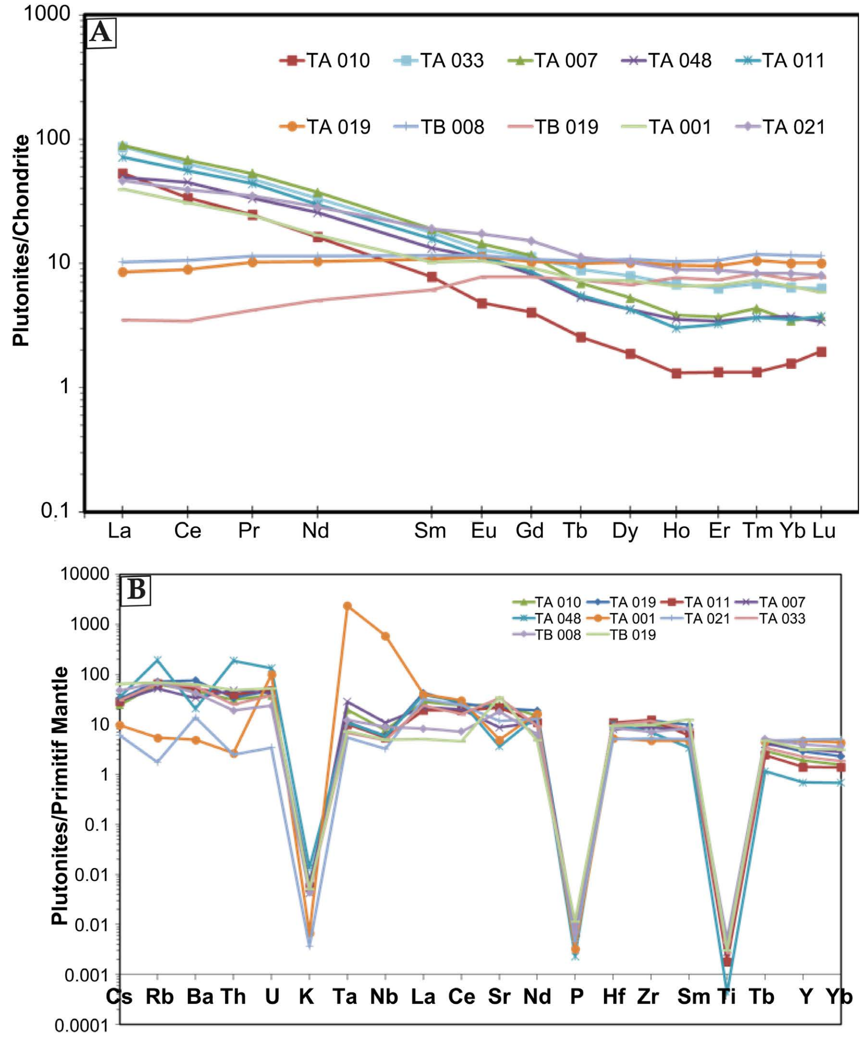


**Figure 5.** Chondrite normalized rare earth spectra and primitive mantle normalized multi-element spectra applied to plutonites of the region of Bondoukou-Tanda.

magmatic evolution of these granites. Negative cerium anomalies (Ce/Ce* = 0.89 - 0.93) are observed. The compositions in trace elements of the granites are reported on the multi-element diagrams normalized to the primitive mantle (**Figure 5(B)**). The profiles are generally similar with an enrichment of lithophile elements (Rb and K). A generally negative anomaly in Ta, Nb, P and Ti is observed. These spectrums have strong Nb negative anomalies but are relatively smaller in Ti, characteristic of magmas relating to subduction zones. The negative anomalies in observed Ti are due to the fractionation of magnetite in the source. Positive and negative anomalies in Sr and Th are observed.

#### 4.2.2. Granodiorite

Granodiorites have $SiO_2$ contents from 68.79% to 69.98% and alkaline ($Na_2O$ + $K_2O$) from 6.03% to 7.27%. Their respective contents in $Al_2O_3$ and MgO vary from 14.43% to 15.72% and from 0.81% to 1.74%, with (Mg#) = 40.22% to 48.36%. Their $TiO_2$ value is very low (0.33% to 0.42%). They belong to the calco-alcaline series (**Figure 3(B)**). The REE contents (ΣREE) of the granodiorites are between 75.72 ppm and 125.50 ppm. The rare earth spectrum of these normalized rocks in chondrites according to (Sun & Mc.donough, 1995) (**Figure 5(A)**), are on average slope with a fractionation of: [$(La/Sm)_N$ = 3.05 - 4.74; $(La/Yb)_N$ = 13.21 - 25.86]. These rocks generally have trends in positive for negatives in Europium (Eu/Eu* = 0.97 - 1.16) and in cerium (Ce/Ce* = 0.79 - 1.15). These trends of positive and negative anomalies in Europium and Cerium are probably due to a divergence in the magmatic evolution of these rocks. The concentrations of elements in traces in the granodiorites of the region of Bondoukou-Tanda are as follows: the Ba (312 - 665 ppm), Co (6 - 12.37 ppm), Cu (9.7 - 45.86 ppm), V (33 - 69.71 ppm), Y (6.41 - 13.13 ppm), Ce (34.74 - 55.3 ppm), Zr (102.4 - 138.7 ppm), Rb (41.63 - 52.48 ppm), and Zn (36 - 58.44 ppm). Their U contents (0.87 - 1.70 ppm), Th (2.86 - 4.90 ppm), Hf (2.90 - 3.38 ppm), and Nb (3.88 - 5.30 ppm) are weak. The compositions in trace elements of the granodiorites reported on the multi-element diagrams normalized to the primitive mantle (**Figure 5(B)**). These profiles are generally similar, marked by a general enrichment of lithophile elements (Cs, Rb, and K) and negative anomalies of Nb-Ta. The geochemical devices observed such as the enrichment in LILE and the marked negative anomalies of Nb-Ta are characteristic of the magmas relating to the subduction emplacement. Negative Ti observed anomalies are due to the fractionation of magnetite in the source.

#### 4.2.3. Tonalite

$SiO_2$ and alkaline contents ($Na_2O + K_2O$) of Tonalites vary from 63.31% to 70.10% and from 6.10% to 6.77% (**Figure 3(A)**). $AL_2O_3$ varies from 15.36% to 16.24%; $TiO_2$ varies from 0.33% to 0.60%; and MgO varies from 1.05% to 2.33%, with (Mg#) = 41.02 - 45.32. The REE contents (ΣREE) of the tonalites are between 91.24 ppm and 425.8 ppm. The spectrum of the rare earth elements of these rocks normalized at the chondrites according to Sun & McDonough (1995), presented in (**Figure 5(A)**). These contents are around 4 to 429 times the chondrite content. The fractionation is: [$(La/Sm)_N$ = 3.02 - 4.26; $(La/Yb)_N$ = 13.19 - 23.33]. These rocks generally have a very slightly positive negative anomaly in Europium (Eu/Eu* = 0.90 - 1.06). Negative cerium anomalies (Ce/Ce* = 0.33 - 0.99) are observed. The compositions in elements in traces of the tonalites, reported on the multi-element diagrams to the primitive mantle (**Figure 5(B)**), show significant enrichments in LILES (Cs, Ba, Rb, U) and LREEs (La, Ce, Pr, Nd and Sm) relative to HFSE (Ta, Zr, Hf and Y) and HREE (Tb, Dy, Ho, Er, Tm, Yb and Lu). A generally negative anomaly in K, Nb, P and TI is observed. These enrichments thus the negative anomalies observed reflect the characteristics of the magmas relating to the subduction. The negative anomalies in observed Ti are due to the fractionation of magnetite and titanite in the source.

#### 4.2.4. Gabbro

Gabbros are characterized by $SiO_2$ contents from 47.48% to 52.88%, in alkaline

($Na_2O + K_2O$) from 1.81% to 3.62%, in $AL_2O_3$ from 14.80% to 17.26% and in $TiO_2$ from 0.60% to 0.93%. $Fe_2O_3$ varies 9.61% to 11.89% and MnO is between 0.12% and 0.19%. MgO values are between 4.5% and 6.93%, with (Mg#) = 51.39% - 60.12%. The REE contents (ΣREE) of the gabbros vary from 17.86 to 62 ppm. As reported on normalized chondrites diagrams (Sun and McDonough, 1995); (**Figure 5(A)**), the rare earth spectrum is depleted in LREE with a very low fractionation: $(La/Sm)_N$ = 0.57 - 3.89 and $(La/Yb)_N$ = 0.47 - 6.07. These rocks show positive anomalies in Europium (Eu/Eu* = 1.08 - 1.17) We observe negative to positive anomalies in cerium (Ce/Ce* = 0.90 - 1). The compositions in trace elements of the normalized gabbros with primitive mantles (**Figure 5(B)**) show generally similar spidergrams. The spectrum of these rocks shows a slight enrichment in LILE (Cs and Rb), positive anomalies in Ta and negative Nb, K, Ti and P.

#### 4.2.5. Diorite

Diorites have $SiO_2$ contents from 57.91% to 58.07% and alkaline ($Na_2O + K_2O$) from 4.37% to 5.28%. $Al_2O_3$ varies from 14.85% to 15.97% and MgO from 3.22% to 5.24%, with (Mg#) = 46.21 to 62.84. Their $TiO_2$ values are low (0.60%). Diorites are calco-alkaline. The REE contents (ΣREE) of the Diorites are between 85.02 and 167.7 ppm. The spectrum of the rare earth elements of these normalized rocks with chondrites according to Sun & Mc. Donough (1995) (**Figure 5(A)**) shows a fractionation of: [$(La/Sm)_N$ = 2.44 - 3.80; $(La/Yb)_N$ = 5.57 - 15.12]. These contents are around 6 to 76 times the chondritic content. These rocks have negative anomalies of almost zero in Europium (Eu/Eu*) = 0.89 - 1.02. Anomalies almost zero in cerium (Ce/Ce* = 0.97) are observed. The spectrum of normalized diorites with primitive mantle (**Figure 5(B)**) is marked by an enrichment of lithophile elements (Cs, Ba, U, Sr and Ta). The most characteristic features are the clear negative anomalies in Nb, characteristic of the magmas enriched in the mantle during an episode of subduction. The negative anomalies in Ti, K and P that we find are due to the fractionation of magnetite, potassium feldspars and sphenes in the source.

## 5. Discussion

### 5.1. Magmatic Evolution and Source of Magma

The intrusives of the Bondoukou-Tanda region are granites, granodiorites, tonalites, gabbros and diorites. The petrographic study highlights evidence of intense hydrothermal alteration undergone by these facies. These are mainly sericitization, chloritization and epidotation induced by epizonal metamorphism like the intrusives of the Baoulé-Mossi domain (Vidal et al., 2009; Baratoux et al., 2011). Still on the petrographic level, we have noticed that the granodiorites express an extreme poverty in potassium feldspars which reflects their placement during deformation. These rocks evolved by fractional crystallization, hence their enrichment in Rb and their depletion in Sr. The Ba and Sr anomalies in the spectrum suggest that feldspars are present in the residual liquid and the negative P anomaly is the result of apatite fractionation. The high Ba contents compared to the Sr show that there was an important fractionation of plagioclase in the rock. The meta-aluminous to peraluminous trends in terms of the chemistry of these intrusives clearly show that they issued a hybrid source (mantle-crust). Structured by Eoeburnean magmatism, these massifs are similar to the geological formations of Boromo-Houndé and Banfora in Burkina Faso (Parra-Avila et al., 2018). They are also calc-alkaline and highly enriched in LREE. Indeed, for (Barbarin, 1990), granitoids with these characteristics have a hybrid origin (mantle and crustal). According to Rogers & Hawkesworth (1989), Sigmarsson et al. (1990), the presence of residual garnet and/or hornblende explains the low Yb contents of the magmas. The $(La/Yb)_N$ ratios between 0 and 40 and $Yb_N$ levels between 0 and 5 ppm observed in these samples support this assertion. This is also explained by the fact that it is type I. The low $TiO_2$ contents of the gabbros analyzed resemble those of the plutonic rocks of the magmatic arcs (Pearce & Cann, 1973), but are different from the basalts of those of the intra-plaque arrangements, which often maintain the high $TiO_2$ concentrations (>2%). The rare earth elements spectrum of Bondoukou-Tanda region intrusives is generally show negative to almost zero anomalies in europium, with however very rare slightly positive anomalies. Indeed, for Martin (1999), the absence of an anomaly in Eu would come from the fusion of a hydrated subducted oceanic crust in a moderately deep subduction zone which reacted with the mantle at the base of the continental crust. Cerium anomalies are common to modern arc magmas but can also result from post-magmatic alterations such as the dominant circulation of hydrothermal fluids (Abouchami et al., 1990; Sylvester & Attoh, 1992).

### 5.2. Tectonic Implication

**Figure 6(A)** shows that the granitoides of the Bondoukou-Tanda region are generally put in place in a context of volcanic arc, according to the diagram of Pearce et al., 1984. In the diagram the/yb-yb of Martin (1986), in the **Figure 6(b)**, these rocks are generally located in the common field with archaean TTG and rocks of the island arcs. This position of these rocks shows that they have a certain affinity for the Archaean TTG. This shows a possibility of mixing due to the existence of a small archaean inherited component. Proponents of the arc-type setting across the Baoulé-Mossi domain have identified whole-rock elemental compositions which are commonly associated with modern arc environments. These include negative Nb and Ta anomalies and variable degrees of enrichment of the LILE (Arculus et al., 1999). Recent studies have identified subduction-related geochemical signatures across Burkina Faso, Ghana, Guinea and Mali (Fontaine et al., 2017; Lambert-Smith et al., 2016; Masurel et al., 2017; Petersson et al., 2016). Furthermore, these rocks exhibit a highly fractionation spectrum in the HREE portion, which is typical of most subduction zones. The intrusives of the Bondoukou-Tanda region show an enrichment in lithophilic elements (LILE), a depletion in HFSE elements, as well as a clear negative anomaly in Nb-Ta. According to (Doumbia et al., 1998), these characteristics observed on

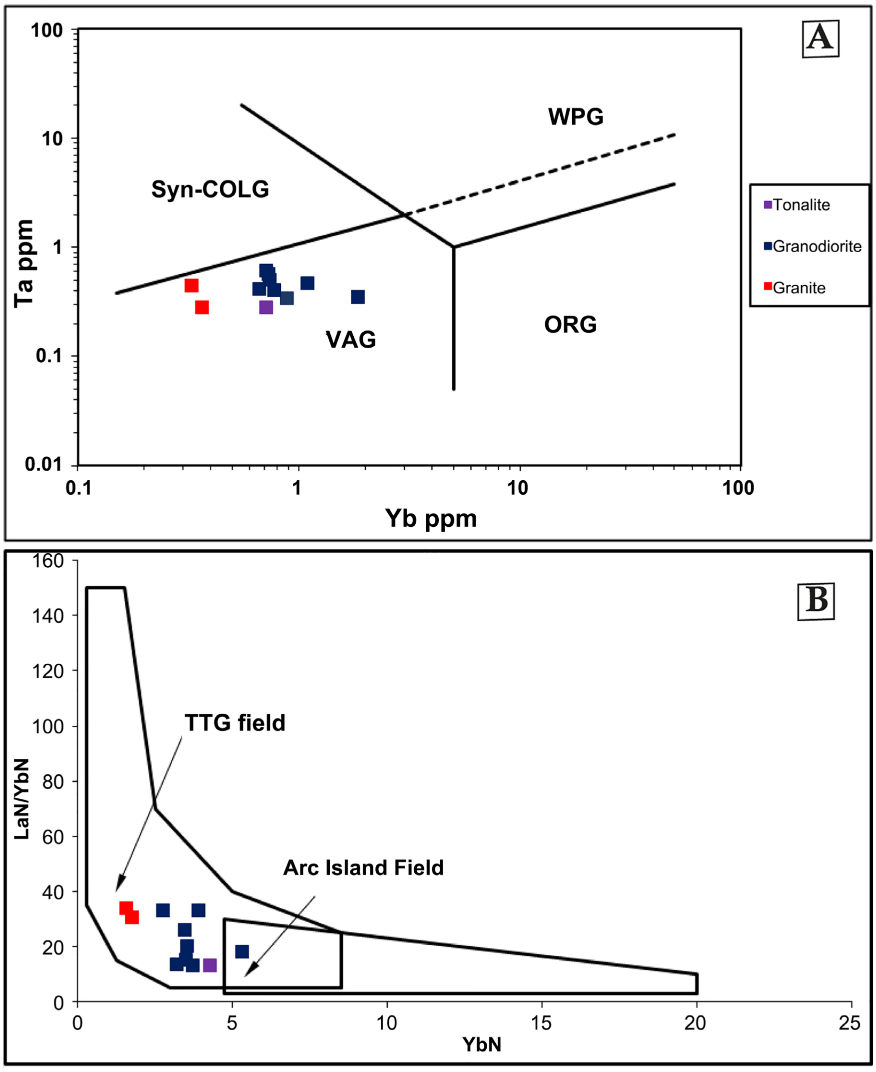


**Figure 6.** (A) Ta vs Yb diagram from Pearce et al., 1984 and (B) La/Yb-Yb diagram from Martin (1986) applied to granitoids in the Bondoukou-Tanda region.

these intrusives imply that they would have been emplacement in active continental margins. Significant negative Nb anomalies also indicate the role played by titaniferous and/or amphibole phases (Martin, 1999). Positive Ta and negative Nb, K, Ti and P anomalies clearly indicate a subduction environment more precisely in arc type.

## 6. Conclusion

The Bondoukou-Tanda intrusives are divided into four main facies which are granites, granodiorites, tonalites, gabbros and diorites. These formations of the Baoulé-Mossi domain structured by the Eburnean orogenic mega cycle are affected by hydrothermalism, particularly sericitization, chloritization and epidotation which characterize the epizonal metamorphic facies which facies is frequent at the level of the rocks of the West African craton. These resulting from the Eoeburnean magmatism have evolved by the process of fractional crystallization also confirmed by geochemical data. Regarding their source, the intrusives of the study area have a hybrid origin, hence their chemistry, which varies from metaluminous to peraluminous. Concerning the geotectonic context, the arguments of geochemistry show that these formations define an emplacement by the mechanism of subduction more precisely in an arc context as the majority of the rocks of the West African craton.

## Conflicts of Interest

The authors declare no conflicts of interest regarding the publication of this paper

## References

Abouchami, W., Boher, M., Michard, A., & Albared, F. (1990). A Major 2.1 Ga Event of Mafic Magma Tism in West Africa: An Early Stage of Crustal Accretion. *Journal of Geophysical Research: Solid Earth, 95,* 605-617. https://doi.org/10.1029/JB095iB11p17605

Allibone, A., McCuaig, T. C., Harris, D., Etheridge, M., Munroe, S., & Byrne, D. (2002). Structural Controls on Gold Mineralization at the Ashanti Gold Deposit, Obuasi, Ghana. In R. J. Goldfarb, & R. L. Nielsen (Eds.), *Special Publication 9: Integrated Methods for Discovery: Global Exploration in the Twenty-First Century* (pp. 65-93). Society of Economic Geologists. https://doi.org/10.5382/SP.09.04

Arculus, R. J., Lapierre, H., & Jaillard, É. (1999). Geochemical Window into Subduction and Accretion Processes: Raspas Metamorphic Complex, Ecuador. *Geology, 27,* 547-550. https://doi.org/10.1130/0091-7613(1999)027<0547:GWISAA>2.3.CO;2

Baratoux, L., Metelka, V., Naba, S., Jessell, W. M., Gregoire, M., & Ganne, J. (2011). Juvenile Paleoproterozoic Crust Evolution during the Eburnean Orogeny (~2.2 - 2.0 Ga), Western Burkina Faso. *Precambrian Research, 191,* 18-45. https://doi.org/10.1016/j.precamres.2011.08.010

Barbarin, B. (1990). Granitoids: Main Petrogenetic Classifications in Relation to Origin and Tectonic Setting. *Geological Journal, 25,* 227-238. https://doi.org/10.1002/gj.3350250306

Boher, M., Abouchami, W., Michard, A., Albarède, F., & Arndt, N. T. (1992). Crustal Growth in West Africa at 2.1 Ga. *Journal of Geophysical Research: Solid Earth, 97,* 345-369. https://doi.org/10.1029/91JB01640

Castaing, C., Billa, M., Milesi, J., Thiéblemont, D., Le Métour, J., Egal, E., Donzeau, M. (BRGM) (coordonnateurs), G. C., Cocherie, A., Chèvremont, P., Tegyey, M., Itard, Y. (BRGM), Zida, B., Ouedraogo, I., Kote, S., Kabore, B. E., Ouedraogo, C. (BUMIGEB), Ki, J.C., & Zunino, C. (ANTEA) (2003). *Notice explicative de la carte geólogique et miniére du Burkina Faso 1/1,000,000* (p. 147). Bureau de Recherches Géologiques et Minières.

Chappell, B. W., & White, A. J. R. (1974). Two Contrasting Granite Types. *Pacific Geology, 8,* 173-174.

De Kock, G. S., Armstrong, R. A., Siegfried, H. P., & Thomas, E. (2011). Geochronology of the Birim Supergroup of the West African Craton in the Wa-Bolé Region of West-Central Ghana: Implications for the Stratigraphic Framework. *Journal of African Earth Sciences, 59,* 1-40. https://doi.org/10.1016/j.jafrearsci.2010.08.001

Delor, C., Siméon, Y., & Vidal, M. (1995). Peri-Plutonic Gravity Driven Deformations and Transcurrent Leetonics between 2.2 and 2.1 b y: A Case Study from the Birimian

Cycle in Ivory Coast (102 p). *VIII EUG Meeting Abstracts Suppl. Terra Nova,* Vol. 4, Strasbourg.

Doumbia, S., Pouclet, A., Kouamelan, A., Peucat, J. J., Vidal, M., & Delor, C. (1998). Petrogenesis of Juvenile-Type Birimian (Paleoproterozoic) Granitoids in Central Côte d'Ivoire, West Africa: Geochemistry and Geochronology. *Precambrian Research, 87,* 33-63. https://doi.org/10.1016/S0301-9268(97)00201-5

Egal, E., Thiéblemont, D., Lahondère, D., Guerrot, C., Costea, C. A., Iliescu, D., Delor, C., Goujou, J.-C., Lafon, J. M., Tegyey, M., Diaby, S., & Kolié, P. (2002). Late Eburnean Granitization and Tectonics along the Western and Northwestern Margin of the Archean Kénéma-Man Domain (Guinea, West African Craton). *Precambrian Research, 117,* 57-84. https://doi.org/10.1016/S0301-9268(02)00060-8

Feybesse, J.-L., Billa, M., Guerrot, C., Duguey, E., Lescuyer, J.-L., Milesi, J.-P., & Bouchot, V. (2006). The Paleoproterozoic Ghanaian Province: Geodynamic Model and Ore Controls, Including Regional Stress Modeling. *Precambrian Research, 149,* 149-196. https://doi.org/10.1016/j.precamres.2006.06.003

Fontaine, A., Eglinger, A., Ada, K., André-Mayer, A.-S., Reisberg, L., Siebenaller, L., Le Mignot, E., Ganne, J., & Poujol, M. (2017). Geology of the World-Class Kiaka Polyphase Gold Deposit, West African Craton, Burkina Faso. *Journal of African Earth Sciences, 126,* 96-122. https://doi.org/10.1016/j.jafrearsci.2016.11.017

Gasquet, D., Barbey, P., Adou, M., & Paquette, J. L. (2003). Structure, Sr-Nd Isotope Geochemistry and Zircon U-Pb Geochronology of the Granitoids of the Dabakala Area (Côte d'Ivoire): Evidence for a 2.3 Ga Crustal Growth Event in the Palaeoproterozoic of West Africa? *Precambrian Research, 127,* 329-354. https://doi.org/10.1016/S0301-9268(03)00209-2

Grenholm, M. (2014). *The Birimian event in the baoulé mossi domain (West African Craton)—regional and global context*. Master's Thesis in Geology, Lithosphere and Paleobiosphere Sciences, No. 375 (45 hskp/ECTS), Lund University.

Jessell, M. W., Begg, G. C., & Miller, M. S. (2016). The Geophysical Signatures of the West African Craton. *Precambrian Research, 274,* 3-24. https://doi.org/10.1016/j.precamres.2015.08.010

Lahondère, D., Thiéblemont, D., Tegyey, M., Guerrot, C., & Diabate, B. (2002). First Evidence of Early Birimian (2.21 Ga) Volcanic Activity in Upper Guinea: The Volcanics and Associated Rocks of the Niani Suite. *Journal of African Earth Sciences, 35,* 417-431. https://doi.org/10.1016/S0899-5362(02)00145-8

Lambert-Smith, J. S., Lawrence, D. M., Müller, W., & Treloar, P. J. (2016). Palaeotectonic Setting of the South-Eastern Kédougou-Kéniéba Inlier, West Africa: New Insights from Igneous Trace Element Geochemistry and U-Pb Zircon Ages. *Precambrian Research 274,* 110-135. https://doi.org/10.1016/j.precamres.2015.10.013

Leube, A., Hirdes, W., Mauer, R., & Kesse, G. O. (1990). The Early Proterozoic Birimian Supergroup of Ghana and Some Aspects of Its Associated Gold Mineralization. *Precambrian Research, 46,* 139-165. https://doi.org/10.1016/0301-9268(90)90070-7

Lompo, M. (2009). Geodynamic Evolution of the 2.25-2.0 Ga Palaeoproterozoic Magmatic Rocks in the Man-Leo Shield of the West African Craton. A Model of Subsidence of an Oceanic Plateau. *Geological Society of London Special Publications, 323,* 231-254. https://doi.org/10.1144/SP323.11

Martin, H. (1986). Effect of Steeper Archaean Geothermal Gradient on Geochemistry of Subductionzone Magmas. *Geology, 14,* 753-756. https://doi.org/10.1130/0091-7613(1986)14<753:EOSAGG>2.0.CO;2

Martin, H. (1999). Adakitic Magmas: Modern Analogues of Archean Granitoids. *Lithos,* *46,* 411-429. https://doi.org/10.1016/S0024-4937(98)00076-0

Masurel, Q., Thébaud, N., Miller, J., & Ulrich, S. (2017). The Tectono-Magmatic Framework to Gold Mineralisation in the Sadiola-Yatela Gold Camp and Implications for the Paleotectonic Setting of the Kédougou-Kénieba Inlier, West Africa. *Precambrian Research, 292,* 35-56. https://doi.org/10.1016/j.precamres.2017.01.017

Middlemost, E. A. K. (1994). Naming Materials in the Magma/Igneous Rock System. *Earth-Science Reviews, 37,* 215-224. https://doi.org/10.1016/0012-8252(94)90029-9

Milési, J.-P., Feybesse, J.-L., Pinna, P., Deschamps, Y., Kampunzu, H., Muhongo Lescuyer, J. L., Le Goff, E., Delor, C., Billa, M., Ralay, F., & Heinry, C. (2004). Geological Map of Africa 1:10,000,000, SIGAfrique Project. In *20th Conference of African Geology*. Orléans: Bureau de Recherches Géologiques et Minières.

Naba, S., Lompo, M., Debat, P., Bouchez, J. L., & Beziat, D. (2004). Structure and Emplacement Model for Late-Orogenic Paleoproterozoic Granitoids: The Tenkodogo-Yamba Elongate Pluton (Eastern Burkina Faso). *Journal of African Earth Sciences, 38,* 41-57.

Parra-Avila, L. A., Belousova, E., Fiorentini, M. L., Eglinger, A., Block, S., & Miller, J. (2018) Zircon Hf and O-isotope Constraints on the Evolution of the Paleoproterozoic Baoulé-Mossi Domain of the Southern West African Craton. *Precambrian Research, 306,* 174-188. https://doi.org/10.1016/j.precamres.2017.12.044

Parra-Avila, L. A., Kemp, A. I. S., Fiorentini, M. L., Belousova, E., Baratoux, L., Block, S., Jessell, M., Bruguier, O., Begg, G. C., Miller, J., Davis, J., & McCuaig, T. C. (2017). The Geochronological Evolution of the Paleoproterozoic Baoulé-Mossi Domain of the Southern West African Craton. *Precambrian Research, 300,* 1-27. https://doi.org/10.1016/j.precamres.2017.07.036

Pearce, J. A., & Cann J. R. (1973). Tectonic Setting of Basic Volcanic Rocks Determined Using Trace Element Analyses. *Earth and Planetary Science Letters, 19*, 290-300. https://doi.org/10.1016/0012-821X(73)90129-5

Petersson, A., Scherstén, A., Kemp, A. I. S., Kristinsdóttir, B., Kalvig, P., & Anum, S. (2016). Zircon U-Pb-Hf Evidence for Subduction Related Crustal Growth and Reworking of Archaean Crust within the Palaeoproterozoic Birimian Terrane, West African Craton, SE Ghana. *Precambrian Research, 275,* 286-309. https://doi.org/10.1016/j.precamres.2016.01.006

Pouclet, A., Doumbia, S., & Vidal, M. (2006). Geodynamic Setting of the Birimian Volcanism in Central Ivory Coast (Western Africa) and Its Place in the Paleoproterozoic Evolution of the Man Shield. *Bulletin de la Société Géologique de France, 177,* 105-121. https://doi.org/10.2113/gssgfbull.177.2.105

Rocci, G. (1965). Essai D'interprétation Des Mesures Géochronologiques de la Structure De L'ouest Africain. *Science de la Terre, 10,* 461-479.

Rogers, G., & Hawkesworth, C. J. (1989). A Geochemical Traverse across the North Chilean Andes: Evidence for Crust Generation from the Mantle Wedge. *Earth and Planetary Science Letters, 91,* 271-285. https://doi.org/10.1016/0012-821X(89)90003-4

Shand, S. J. (1922). The Problem of the Alkaline Rocks. *Proceedings of the Geological Society of South Africa, 25,* 19-33.

Sigmarsson, O. et al. (1990). Uranium and $^{10}$Be Enrichments by Fluids in Andean Arc Magmas. *Nature, 346,* 163-165. https://doi.org/10.1038/346163a0

Siméon, Y., Delor C., Zeade Z., Kone Y., Yao B., Vidal, M., Diaby I., Konan, G., Dje B. I., N'da, D., Dommanget, A., Cautru, J. P., Guerrot, C., & Chiron, J.-C. (1995). *Notice explicative de la cartegéologique de la Côte d'Ivoire à 1/200 000, feuille Agnibilékro* (No. 8). Mémoire de la Direction des Mines et de la Géologie de la Côte d'Ivoire.

Sun, S. S., & McDonough, W. F. (1995). The Composition of the Earth. *Chemical Geology, 120,* 223-253. https://doi.org/10.1016/0009-2541(94)00140-4

Sylvester, P. J., & Attoh K. (1992). Lithostratigraphy and Composition of 2.1 Ga Greenstone Belts of the West African Craton and Their Bearing on Crustal Evolution and Archean-Proterozoic boundary. *The Journal of Geology, 100,* 377-393. https://doi.org/10.1086/629593

Tapsoba, B., Lo, C. H., Jahn, B. M., Chung, S. L., Wenmenga, U., & Iizuka, Y. (2013). Chemical and Sr-Nd Isotopic Compositions and Zircon U-Pb Ages of the Birimian Granitoids from NE Burkina Faso, West African Craton: Implications on the Geodynamic Setting and Crustal Evolution. *Precambrian Research, 224,* 364-396. https://doi.org/10.1016/j.precamres.2012.09.013

Tempier, P. (1969). Données récentes sur la géologie de socle de la Côte d'Ivoire. *Annales de l'Université d'Abidjan (Côte d'Ivoire), 5,* 55-92.

Toure, S. (2007). *Pétrologie et géochronologie du massif granitoïde de Bondoukou, Nord-Est de la Côte d'Ivoire. Évolution magmatique et contexte géodynamique au Protérozoïque inférieur. Relations avec le volcano-détritique du Zanzan, Koun, Tanda, attribué au Tarkwaïen du Ghana* (224p). Implications paléogéographiques. Thèse de Doctorat Es Nat., Univ. d'Abobo Adjamé.

Toure, S., Caen-Vachette, M., &Tempier, P. (1987). Nouvelles données pétrographiques, géochimiques et géochronologiques du massif "granitique" de Bondoukou (Côte d'Ivoire) mise en évidence d'un âge Burkinien, par isochrone Rb/Sr sur roches totales. *Journal of African Earth Sciences, 6,* 269-274. https://doi.org/10.1016/0899-5362(87)90068-6

Tshibubudze, A., Hein, K. A. A., Peters, L. F. H., Woolfe, A. J., & McCuaig, T. C. (2013). Olest UPb Crystallisation age for the West African Craton from the Oudalan-Gorouol belt of Burkina Faso. *South African Journal of Geology, 116,* 169-181. https://doi.org/10.2113/gssajg.116.1.169

Vegas, N., Naba, S., Bouchez, J. L., & Jessell, M. (2008). Structure and Emplacement of Granite Plutons in the Paleoproterozoic Crust of Eastern Burkina Faso: Rheological Implications. *International Journal of Earth Sciences, 97,* 1165-1180. https://doi.org/10.1007/s00531-007-0205-z

Vidal, M., Gumiaux, C., Cagnard, F., Pouclet, A., Ouattara, G., & Pichon, M. (2009). Evolution of a Paleoproterozoic "Weak Type" Orogeny in the West African Craton (Ivory Coast). *Tectonophysics, 477,* 145-159. https://doi.org/10.1016/j.tecto.2009.02.010

Wright, J. B., Hastings, D. A., Jones, W. B., & Williams, H. R. (1969). *Geology and Mineral Resources of West Africa*. London: Allen &Unwin (Editeurs), 187 p.

Zeade, Z., Delor C, Simeon, Y., Yao, B D., Vidal, M., Sonnendrucker, P., Diaby, I., & Cautru, J. P. (1995). *Notice explicative de la carte Géologique de la Côte d'Ivoire 237 à 1/200000, Feuille Bondoukou* (No. 10). Mémoire de la Direction des Mines et de la Géologie de la Côte d'ivoire.